Aggregation-fragmentation-diffusion model for trail dynamics

Kyle Kawagoe,[1,2] Greg Huber,[1] Marc Pradas,[3,1] Michael Wilkinson,[3,1] Alain Pumir,[4,1] and Eli Ben-Naim[5]
[1]*Kavli Institute for Theoretical Physics, University of California Santa Barbara, California 93106, USA*
[2]*Department of Physics, University of Chicago, Chicago, Illinois 60637, USA*
[3]*School of Mathematics and Statistics, The Open University, Walton Hall, Milton Keynes MK7 6AA, England*
[4]*Laboratoire de Physique, Ecole Normale Supérieure de Lyon, CNRS, Université de Lyon, F-69007 Lyon, France*
[5]*Theoretical Division and Center for Nonlinear Studies, Los Alamos National Laboratory, Los Alamos, New Mexico 87545, USA*
(Received 15 May 2017; published 21 July 2017)

We investigate statistical properties of trails formed by a random process incorporating aggregation, fragmentation, and diffusion. In this stochastic process, which takes place in one spatial dimension, two neighboring trails may combine to form a larger one, and also one trail may split into two. In addition, trails move diffusively. The model is defined by two parameters which quantify the fragmentation rate and the fragment size. In the long-time limit, the system reaches a steady state, and our focus is the limiting distribution of trail weights. We find that the density of trail weight has power-law tail $P(w) \sim w^{-\gamma}$ for small weight w. We obtain the exponent γ analytically and find that it varies continuously with the two model parameters. The exponent γ can be positive or negative, so that in one range of parameters small-weight trails are abundant and in the complementary range they are rare.

DOI: 10.1103/PhysRevE.96.012142

I. INTRODUCTION

Processes by which objects may randomly merge or split into smaller parts are found in a wide range of natural and physical phenomena [1–6], including reversible polymerization [7–9], river networks [10,11], and force chains [12,13]. Irreversible aggregation can lead to gelation where a single aggregate forms and accounts for a finite fraction of system mass [14–18], and irreversible fragmentation can result in shattering where zero-mass fragments account for a finite fraction of all mass [19–23]. When aggregation and fragmentation compete, the system typically reaches a steady state, and the precise balance between merger and breakup controls the nature of the steady state [4,5,9].

Many studies of aggregation-fragmentation processes do not implicitly account for aggregate mobility, nor do these models allow for an underlying spatial structure [1]. In this paper we investigate a stochastic process in which trajectories, which we call "trails," can diffuse, merge, or split. The trajectories each carry a "weight," or population, and the process can serve as a model for migration trails of animals [24,25]. The current investigation complements recent studies of chaotic dynamics [26,27] which reveal distinctive trajectories, which have qualitative and quantitative similarities to the trails which are investigated here.

The stochastic process for the evolution of trails takes place in one spatial dimension. In our model, both space and time are discrete. At each time step, every trail may split, with probability p, into two smaller trails or remain intact with the complementary probability $1 - p$ (see Fig. 1). In the former case, two trails are created with weights that are fractions r and $1 - r$ of the weight of the parent trail, and, hence, the overall weight is conserved. Trails also move randomly, and essentially perform a simple random walk. Finally, when two trails collide, they merge, with the overall weight being a conserved quantity.

Regardless of the initial conditions, the system evolves toward a steady state. We study the steady-state density $P(w)$ of trails with weight w and find the power-law behavior,

$$P(w) \sim w^{-\gamma}, \tag{1}$$

for small weights, $w \to 0$. Interestingly, the power-law exponent varies continuously with the fragmentation probability p and the fragmentation ratio r as γ is a real root of the equation

$$r^{\gamma-1} + (1-r)^{\gamma-1} = \frac{3-p}{1-p}. \tag{2}$$

Results of our numerical simulations are in excellent agreement with this theoretical prediction. Depending on the parameters p and r, the exponent $\gamma < 1$ can be positive such that small-weight trails are enhanced, or it can be negative such that small-weight trails are suppressed. Our theoretical approach assumes that spatial correlations are absent at the steady state, and our extensive numerical simulations support this assumption.

The rest of this paper is organized as follows. Section II introduces the model, and Sec. III provides an elementary derivation of the trail concentration. In Sec. IV, we analyze the density of trail weights theoretically and numerically. We obtain analytic expressions for moments of the trail density and also obtain the distribution of small weights. Section V addresses the weak fragmentation limit where aggregation and fragmentation proceed independently. In this limit, dynamical properties of voids between adjacent trails can be understood using first-passage properties of an ordinary random walk. We conclude in Sec. VI.

II. THE MODEL

Our aggregation-fragmentation-diffusion model takes place on an unbounded lattice in one dimension. A lattice site labeled i may be either vacant or occupied by a trail with weight w_i. The weight can also be understood as the density of a trail of particles concentrated at location i. In the initial configuration, each site is occupied by a trail with weight unity.

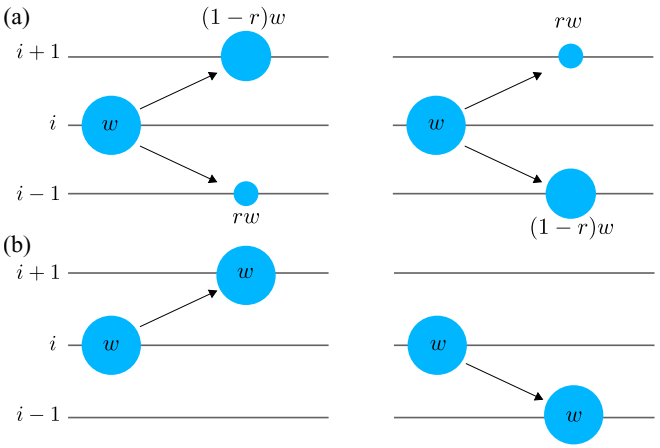

FIG. 1. Illustration of (a) fragmentation with probability p, with a fixed ratio between the two fragments, characterized by r, and (b) random hopping with probability $1-p$.

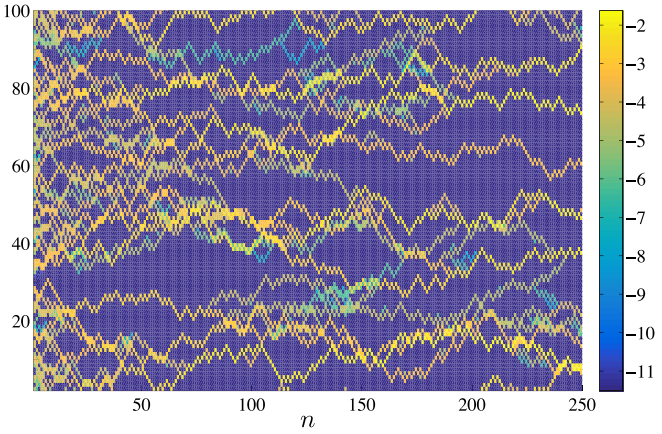

FIG. 2. A numerical realization of the aggregation-fragmentation-diffusion process with $r = 0.01$ and $p = 0.05$. The color coding illustrates weights from low (blue) to high (yellow) values, and the color bar is in natural logarithmic scale. Unoccupied sites are dark purple.

The stochastic process has three elements. (i) *Fragmentation*. With the probability p, a trail with weight w_i splits into two fragments with weights rw_i and $(1-r)w_i$. One of these fragments moves to neighboring site $i-1$ and the remaining fragment moves to neighboring site $i+1$. The two realizations are equally likely (see Fig. 1). (ii) *Diffusion*: With the complementary probability $1-p$ the trail remains intact and it moves, with equal probabilities, to site $i-1$ or to site $i+1$. (iii) *Aggregation*. All sites are updated simultaneously according to the fragmentation and diffusion steps above. When two distinct trails arrive at the same site, they immediately merge to form a new trail whose weight equals the sum of those of the two original trails.

Hence, two parameters characterize the model: the fragmentation probability, p, with $0 < p < 1$, and the fragmentation ratio, r, with $0 < r < 1$. These parameters control how the weight at each site evolves prior to the final aggregation step,

$$w \to \begin{cases} rw,(1-r)w & \text{with probability } p, \\ w & \text{with probability } 1-p. \end{cases} \tag{3}$$

All trails are updated simultaneously, and time n is augmented by one after each iteration, $n \to n+1$. Essentially, trails perform a random walk (see Fig. 2), and importantly, mobility is not coupled to weight. We stress that total trail weight is conserved since both fragmentation and aggregation are conservative processes.

Our Monte Carlo simulations were performed using a regular lattice with N sites and periodic boundary conditions. Initially, each site is occupied with a trail of unit weight. In each iteration, all sites are updated simultaneously according to the model rules. Namely, a trail jumps without splitting to a neighboring site, with probability $1-p$, or decomposes into two fragments, with probability p, as in Fig. 1 and Eq. (3). Two trails landing at iteration n at the same location immediately merge. Figure 2 shows trajectories in a space-time diagram using simulation data.

III. THE CONCENTRATION

We first study the trail concentration c, defined as fraction of occupied sites. Our primary focus is the steady state, where the competing processes of aggregation and fragmentation balance each other. The fragmentation ratio r affects the trail weight, but it does not affect the number of trails. Hence, the concentration depends on the fragmentation probability p alone. By assuming that occupations at neighboring sites are not correlated, we can write a closed equation for the concentration. In each fragmentation event a single trail generates two trails and, conversely, in each aggregation event two trails coalesce into one. At the steady state, the gain rate and the loss rate balance,

$$p\,c = \left(\frac{1+p}{2}c\right)^2. \tag{4}$$

The fragmentation rate on the left-hand side is proportional to the concentration c and the fragmentation probability p. The aggregation rate equals the probability that two trails arrive at the same site. The quantity in parentheses is the sum of pc and $\frac{1-p}{2}c$ accounting for trail fragments and intact trails, respectively (see Fig. 1). In writing the quadratic aggregation term in (4), we make the assumption that the occupancy at a site is not correlated with that at its next-nearest neighbor.

Rearranging Eq. (4) we find the trail concentration

$$c = \frac{4p}{(1+p)^2}. \tag{5}$$

Figure 3 shows a comparison of Eq. (5) with numerical simulations of the model. The numerical results indicate that spatial correlations in the trail concentration disappear in the steady state. Qualitatively, the equilibrium concentration of domain walls in the one-dimensional Ising model with single-spin flip dynamics exhibits similar phenomenology [28–30].

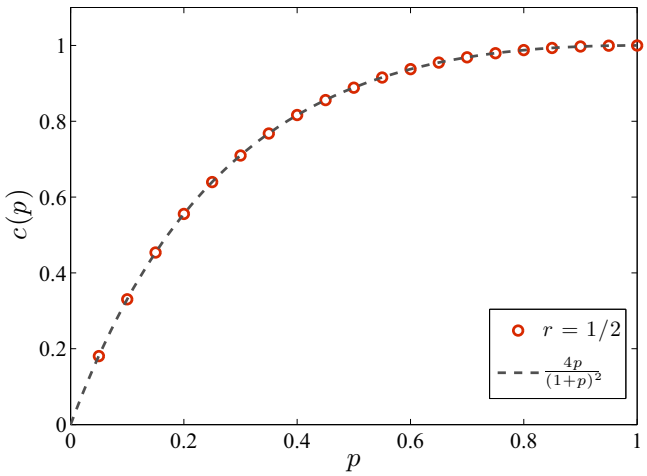

FIG. 3. Numerically computed trail concentration $c(p)$ versus the fragmentation probability p. The dashed line corresponds to the analytic expression (5), and the circles to Monte Carlo simulations on a lattice of $N = 10^6$ sites.

The trail concentration has the following limiting behaviors:

$$c \simeq \begin{cases} 4p & p \to 0, \\ 1 - \frac{1}{4}(1-p)^2 & p \to 1. \end{cases} \quad (6)$$

The concentration vanishes linearly when $p \to 0$, and, hence, the average trail weight, which according to mass conservation is inversely proportional to c, diverges in this limit. Also, the fraction of vacant sites vanishes quadratically when $p \to 1$.

IV. THE WEIGHT DENSITY

We now turn to the main focus of our investigation, the steady-state weight density. Our theory builds on the results of Sec. III, and using the assumption that weights at different sites are not correlated, we can accurately predict key statistical properties of the weight density.

We define the weight density $P(w)$ such that $P(w)dw$ is the fraction of sites occupied by a trail with weight in the infinitesimal range $[w : w + dw]$. Trail weight is conserved throughout the aggregation-fragmentation-diffusion process and, hence, the total weight density $\int dw\, w P(w)$ is a constant. The concentration c equals the integrated weight density

$$c = \int_0^\infty dw P(w). \quad (7)$$

The normalized quantity $c^{-1}P(w)$ is the probability distribution function for the weight.

Changes in trail weight occur in two stages: first, before trails move and, then, after they move. In the first stage, trail weight may change by fragmentation. Let $G(w)$ be the weight density of trails produced at the first stage. According to the random process (3), we have

$$G(w) = \frac{p}{r} P\left(\frac{w}{r}\right) + \frac{p}{1-r} P\left(\frac{w}{1-r}\right) + (1-p)P(w). \quad (8)$$

Here, the first two terms on the right-hand side account for fragments and the last term accounts for intact trails. As also follows from Eq. (8), weight conservation sets $\int dw\, w\, G(w) = \int dw\, w\, P(w)$, and the fragmentation rule (3) implies $\int dw G(w) = (1+p)\int dw P(w)$.

In the steady state, the trail density before an iteration, $P(w)$, is unchanged after one iteration of the combined aggregation-fragmentation diffusion process. This is expressed by the nonlinear-integral equation:

$$P(w) = \left(1 - \frac{1+p}{2}c\right)G(w) + \frac{1}{4}\int_0^w dv\, G(v)G(w-v). \quad (9)$$

The first term on the right-hand side accounts for the scenario where there is no aggregation. It is a product of three factors: (i) the quantity $G(w)/2$, which represents a trail produced at a neighboring site and where the factor $1/2$ accounts for the equal distribution of weight from one site to its two neighbors; (ii) the factor 2 accounting for two neighbors; and (iii) the probability $1 - \frac{1+p}{2}c$ that such a trail avoids aggregation. This probability sums $1 - c$ and $\frac{1-p}{2}c$ for a vacant and an occupied next-nearest neighbor, respectively. The second term on the right-hand side is the aggregation term; it is a convolution of two identical terms of the form $G(w)/2$, with $G(w)$ given by (8). By integrating Eq. (9) over all weights, we recover Eq. (4), and furthermore, this equation is consistent with mass conservation.

We stress that substitution of Eq. (8) into Eq. (9) turns the latter into a closed, nonlinear, equation for the weight density $P(w)$. Compared with Eq. (4), the steady-state equation (8) makes an even stronger assumption that *weights* at different sites are not correlated. Indeed, the convolution term in (9), which accounts for the weight of aggregates, is quadratic in the density $P(w)$.

A. Moment analysis

To examine the validity of this no-correlation assumption, we study the moments of the weight density,

$$M_k = \int dw w^k P(w). \quad (10)$$

Of course, the zeroth moment corresponds to the total concentration $M_0 = c$, and the first moment $M_1 = 1$ corresponds to the total weight density which is a conserved quantity. As shown in Fig. 3, the numerical simulations confirm the predictions of (9) for the zeroth moment.

We now introduce the Laplace transform $M(s) = \int_0^\infty dw e^{-sw} P(w)$, which is the generating function of the moments,

$$M(s) = \sum_{n=0}^{\infty} \frac{(-s)^k}{k!} M_k. \quad (11)$$

By first substituting the concentration (5) into (9), then multiplying Eq. (9) with e^{-sw}, and finally, integrating over weight, we find that the Laplace transform obeys the nonlinear equation

$$M(s) = \frac{1-p}{1+p} U(s) + \frac{1}{4}U^2(s), \quad (12)$$

with $U(s) = pM(rs) + pM(s - rs) + (1-p)M(s)$. The quantity $U(s)$ is the Laplace transform $U(s) = \int dw e^{-sw} G(w)$, and it can be conveniently expressed in terms

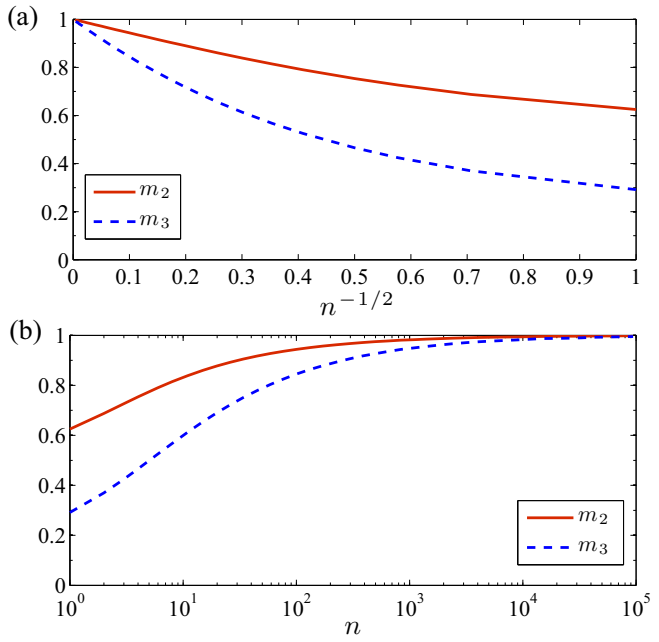

FIG. 4. The normalized second and third moments $m_2(n) = M_2(n)/2$ and $m_3(n) = M_3(n)/6$, versus (a) $n^{-1/2}$ and (b) n. Shown are results of Monte Carlo simulations on a ring with 10^8 sites for the case $r = p = 1/2$. A fourth-order polynomial fit to $m_k(n)$ versus $n^{-1/2}$ yields the asymptotic values 1.0001 and 1.0002 for $m_2(\infty)$ and $m_3(\infty)$, respectively.

of the moments M_k,

$$U(s) = \sum_{n=0}^{\infty} \frac{(-s)^k}{k!} u_k M_k. \tag{13}$$

Here, $u_k = 1 - p[1 - r^k - (1 - r)^k]$, and we quote the values $u_0 = 1 + p, u_1 = 1$, and $u_2 = 1 - 2pr(1 - r)$. Using $M(0) = c$ and $U(0) = (1 + p)c$, we can recover from (12) the trail concentration (5). Mass conservation dictates that M_1 equals the initial mass density. In general, the moments satisfy the recursion

$$M_k = \frac{1}{4(1 - u_k)} \sum_{l=1}^{k-1} \binom{k}{l} u_l u_{k-l} M_l M_{k-l}, \tag{14}$$

when $k \geqslant 2$. In particular, the second and third moments are given by

$$M_2 = \frac{M_1^2}{2(1 - u_2)}, \quad M_3 = \frac{3\, u_2\, M_1^3}{4(1 - u_2)(1 - u_3)}. \tag{15}$$

For the special case $p = r = 1/2$, with $M_1 = 1$, we have $M_0 = 8/9$, $M_2 = 2$, and $M_3 = 6$. Results of our Monte Carlo simulations are in excellent agreement with these theoretical predictions (see Fig. 4). We also verified numerically that (15) holds for other values of the fragmentation probability p and the fragmentation ratio r and for a variety of initial conditions.

We have also examined numerically the empty-interval probability E_l that l consecutive sites are vacant. As expected given the absence of spatial correlations, we confirmed the exponential behavior $E_l = E_1^l$, with $E_1 = 1 - c$ and c given in (5).

We also studied a continuous-time analog of the aggregation-fragmentation-diffusion model with sequential dynamics where sites are updated one at a time. The continuous-time version admits an analytic solution for concentration, but apparently an exact solution for the weight distribution is not feasible. We find that spatial correlations do not vanish, and therefore, qualitative features of the steady state are sensitive to the details of the dynamics.

Below, we discuss the small-weight statistics of the trail density and provide numerical results that confirm the theoretical predictions. Based on the simulation results, we conclude that at the steady state, spatial correlations in trail weight disappear. A similar behavior occurs in adsorption-desorption processes [31–33], where gaps between adsorbed particles in one dimension essentially undergo an aggregation-fragmentation process, and also, in a related model for the propagation of force chains in granular matter [13].

The results of Sec. III imply that in a finite system, every configuration with N_1 occupied sites and N_2 vacant sites is realized with the equilibrium probability $c^{N_1}(1 - c)^{N_2}$ that corresponds to a noninteracting two-state system. The moment analysis indicates that an even stronger statement applies as all states with the same configuration of weights are equally probable. In essence, the weight density $P(w)$ completely describes the system.

B. Small-weight statistics

We now focus on the small-weight tail of the density $P(w)$. In the limit $w \to 0$, the nonlinear terms become negligible. If we substitute the concentration given in (5) into (9), we find that the small-w tail of the steady-state density $P(w)$ satisfies the *linear* equation

$$\frac{1}{r} P\left(\frac{w}{r}\right) + \frac{1}{1 - r} P\left(\frac{w}{1 - r}\right) = \frac{3 - p}{1 - p} P(w). \tag{16}$$

From this equation we arrive at our main result, the power-law behavior $P(w) \sim w^{-\gamma}$, with the exponent γ being root of Eq. (2). Clearly, the exponent $\gamma < 1$ varies continuously with the model parameters r and p. In the special case $r = 1/2$ we have $\gamma = 2 - (\ln \frac{3-p}{1-p})/\ln 2$.

The small-weight statistics also follow from the Laplace transform. When $M(s)$ is small, the nonlinear term in the governing equation (12) is negligible, thereby leading to the linear equation $(1 + p)M(s) = (1 - p)U(s)$. This equation implies the large-s decay $M(s) \sim s^{\gamma-1}$, which is equivalent to the power-law behavior (1), with the exponent γ root of Eq. (2).

Our numerical simulations provide excellent support for Eq. (2). Figure 5 demonstrates the power-law tail of the weight density, and Fig. 6 compares the numerically computed exponent γ for different model parameters with the theoretical prediction.

In a finite system of size N, the power-law tail (1) holds in the range $N^{-1/(1-\gamma)} \ll w \ll 1$. The lower limit follows from the criterion $N \int_0^z dw\, P(w) \sim 1$, which gives an estimate for the scale z of the smallest weight in the system [1]. The scaling law $z \sim N^{-1/(1-\gamma)}$ explains the large variation in the extent of the power-law regime observed in Fig. 5.

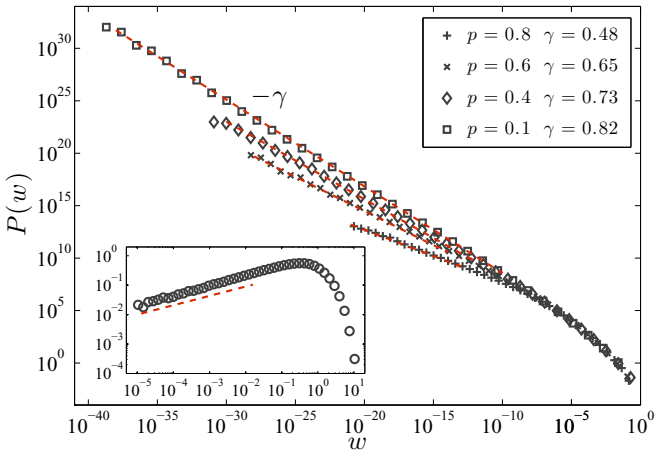

FIG. 5. The power-law tail of the weight density $P(w)$. The curves shown here correspond to different values of p, indicated in the legend, and are obtained from Monte Carlo simulations on a lattice of $N = 10^6$ sites. Dashed lines correspond to the theoretical predictions of Eqs. (1) and (2). The value of r was chosen to be $r = 0.01$. The inset displays the case $r = 0.25$ and $p = 0.7$ for which $\gamma = -0.32$.

Equation (2) implies that there are two distinct regimes of behavior, since the exponent γ vanishes when

$$r(1-r) = \frac{1-p}{3-p}. \tag{17}$$

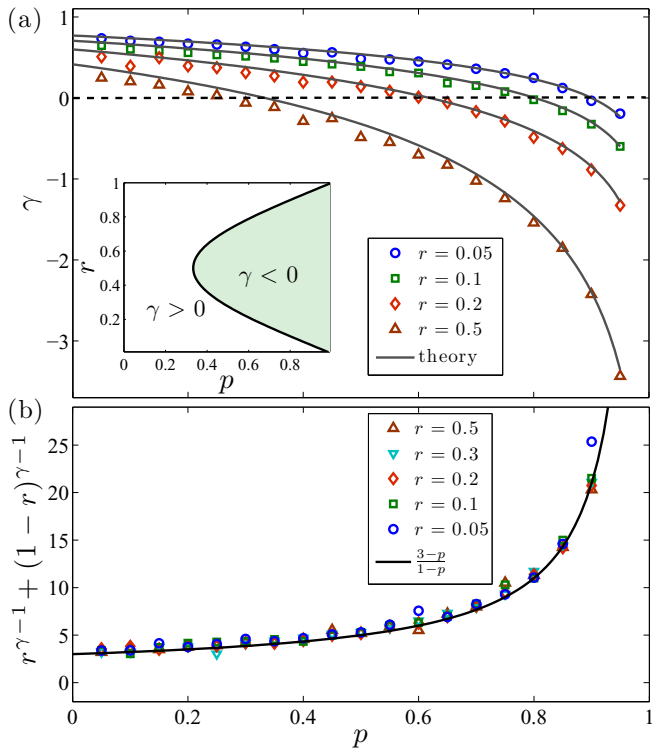

FIG. 6. (a) The exponent γ for different values of p and r. The lines correspond to the theoretical predictions, given by Eq. (2), for different values of r; see the legend. The inset shows the region of negative γ as shaded. (b) When data are plotted as $r^{\gamma-1} + (1-r)^{\gamma-1}$ they collapse into the curve $(3-p)/(1-p)$ (solid line) in accord with (2).

As shown in Fig. 6(a), γ can be positive, in which case, the density of small-weight trails is enhanced. In the complementary regime, γ is negative and small-weight trails are suppressed. When $p < 1/3$ the exponent is always positive, $\gamma > 0$.

The linear equation (16) reflects the nature of the fragmentation process in which weight "cascades" from small trails into even smaller trails according to $w \to rw,(1-r)w$. This cascade process is balanced by aggregation of small trails into larger trails. The power-law behavior is valid over a substantial size range, and throughout this range only terms that are linear in $P(w)$ dominate Eq. (9). Qualitatively similar cascades, where the full nonlinear theory reduces to a linear theory for extreme-value statistics, are found in wave turbulence [34,35] and inelastic gases [36]. Yet, the cascade process described by Eq. (16) has two distinctive features. First, the tail (1) can be vanishing or diverging. Second, in Eq. (9), the term linear in $P(w)$ is also proportional to the trail concentration c. Consequently, the prefactor on the right-hand side of (16) depends on the steady-state value (5) of the concentration, and despite its linear nature, this equation does incorporate a two-point correlation.

For completeness, we mention that we also numerically studied the large-w tail of the weight density. In contrast with the broad power-law tail that may occur at small weights, we find that large weights are exponentially rare, $P(w) \sim \exp(-\text{const.} \times w)$ for $w \gg 1$. This behavior is consistent with the large-size statistics found in irreversible aggregation [18] and in the closely related q model for force chains [12,13].

C. Stochastic fragmentation

The fragmentation process in (3) is deterministic in the sense that the sizes of the two trail fragments are fixed fractions of the original trail. We briefly mention a natural counterpart, stochastic fragmentation, where the fraction $0 < r < 1$ is drawn from the distribution $\eta(r)$. We require that the distribution be (i) normalized $\int_0^1 dr\eta(r) = 1$ and (ii) symmetric $\eta(r) = \eta(1-r)$. It is straightforward to generalize the above theoretical analysis to stochastic fragmentation, and, in particular, Eq. (2) becomes

$$\int_0^1 d\eta\eta(r)[r^{\gamma-1} + (1-r)^{\gamma-1}] = \frac{3-p}{1-p}. \tag{18}$$

For the so-called random-scission model [1,13] where the fraction r is uniformly distributed, $\eta(r) = 1$, we find

$$\gamma = 2\,\frac{1-p}{3-p}. \tag{19}$$

In this case, the exponent γ satisfies $0 < \gamma < 2/3$, and the small-weight tail of the distribution is enhanced, regardless of p.

V. WEAK FRAGMENTATION

We now analyze the small-p case and show that aggregation and fragmentation proceed independently in this regime. In the limit $p \to 0$, the trail concentration vanishes; see Eq. (5), and, consequently, $P(w) \propto p$. By keeping dominant terms of the order $O(p^2)$ and neglecting subdominant terms of the orders

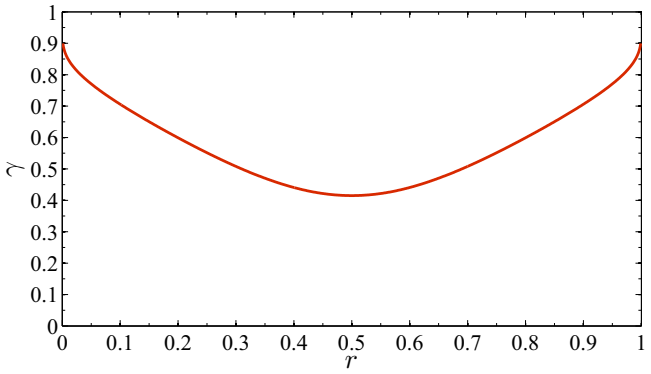

FIG. 7. The exponent γ versus the parameter r for small values of p.

$O(p^3)$ and $O(p^4)$, we find that Eq. (9) simplifies to

$$0 = 4p\left[\frac{1}{r}P\left(\frac{w}{r}\right) + \frac{1}{1-r}P\left(\frac{w}{1-r}\right) - P(w)\right] + \int_0^w dy\, P(y)P(w-y) - 2cP(w). \tag{20}$$

The first two (linear) terms account for fragmentation, while the next two (nonlinear) terms account for aggregation between two intact trails. Thus, fragmentation and aggregation are not coupled when fragmentation is weak. As a check of self-consistency, we integrate (20) to find $c^2 = 4pc$. Hence, the concentration is proportional to the fragmentation probability $c \simeq 4p$ as in (6).

In the limit $w \to 0$, the nonlinear term in Eq. (20) is negligible, and the linear terms satisfy

$$\frac{1}{r}P\left(\frac{w}{r}\right) + \frac{1}{1-r}P\left(\frac{w}{1-r}\right) = 3P(w). \tag{21}$$

This linear equation accepts a solution of algebraic form $P(w) \sim w^{-\gamma}$ for small w, where the exponent $\gamma < 1$ is root of the equation

$$r^{\gamma-1} + (1-r)^{\gamma-1} = 3. \tag{22}$$

Figure 7 shows a plot of $\gamma(r)$ as given by the above equation, where we observe that the minimal value $\gamma = 2 - \frac{\ln 3}{\ln 2}$ is attained when $r = 1/2$.

As discussed above, when fragmentation is weak, the trail concentration is low. Moreover, since fragmentation events are rare, fragmentation and aggregation proceed independently. In this limit, it is relatively simple to characterize the dynamics of voids between adjacent trails. In the limit $p \to 0$, trails merely perform a random walk, and when two trails come to within distance of two sites, there is a finite probability for the two to coalesce. Hence, the problem is equivalent to a first-passage process of a simple random walk (the distance between two independent random walks itself performs a random walk). Let T be the lifetime of a void between two trails and $Q(T)$ be the probability a void has a lifetime T [see Fig. 8(a)]. Using the well-known return probability of a random walk [37], we conclude [see Fig. 8(b)]

$$Q(T) \sim T^{-3/2}. \tag{23}$$

Furthermore, we can also consider the area S of a void in a space-time diagram [see Fig. 8(a)]. Because the edges of the void are random walks, the width of the void scales as $T^{1/2}$ and consequently the area scales as $S \sim T^{3/2}$. Using $R(S)$ for the probability of observing a void with area S, the scaling behavior [see Fig. 8(c)],

$$R(S) \sim S^{-4/3}, \tag{24}$$

follows immediately from (23). Our numerical simulation results, shown in Figs. 8(b) and 8(c), support the first-passage behaviors (23) and (24).

VI. DISCUSSION

We have studied an aggregation-fragmentation-diffusion random process that describes the evolution of trails of particles with local weight density. In our model, a trail may fragment into two or it may stay intact. In addition, trails move randomly, essentially performing diffusion. Aggregation occurs when two trails arrive at the same location. The model is characterized by two parameters: the fragmentation probability, which controls the relative strength of the fragmentation process, and the fragmentation ratio, which controls the size of the produced fragments. An equilibrium state is found, where the two competing processes of aggregation and fragmentation balance each other. In this steady state, the small-weight tail of the fragment density has a power-law tail. The exponent governing this tail varies continuously with the model parameters.

At the core of our theoretical approach are the assumptions that the occupancy and even the weights of trails at different locations are uncorrelated. Our extensive numerical simulations confirm this behavior. The aggregation-fragmentation-diffusion model therefore provides a rare case where a discrete-time model admits an exact solution for the steady-state behavior, despite the fact that the time-dependent behavior involves nontrivial spatial correlations.

Ultimately, the system achieves an equilibrium state, where aggregation and fragmentation are in perfect balance, with the remarkable property that all configurations with the same number of trails are equally probable. Usually, it is possible to trace such behavior to a detailed balance condition where there is zero net flux between any two microscopic configurations of the system. It is an interesting challenge to construct an equivalent condition for our synchronous dynamics.

Interestingly, our numerical results also show that spatial correlations do exist at all times and only at the steady state do they strictly vanish. It is straightforward to convert the steady-state equation (9) into a discrete-time recursion equation for the weight density. Such recursion equation implies fast exponential relaxation toward the steady state, $dM_k/dn \sim \exp[-(1-u_k)n]$ for $k \geqslant 2$. However, our simulations reveal slow algebraic relaxation instead (Fig. 4) $dM_k/dn \sim n^{-3/2}$, for $k \geqslant 2$. Spatial correlations, which steadily diminish with time and eventually disappear altogether, are responsible for slow relaxation toward the steady state. The diffusive relaxation we observe numerically is consistent with the first-passage behavior (23) and is reminiscent of time-dependent behavior in reaction-diffusion processes involving aggregation in one spatial dimension [38–40].

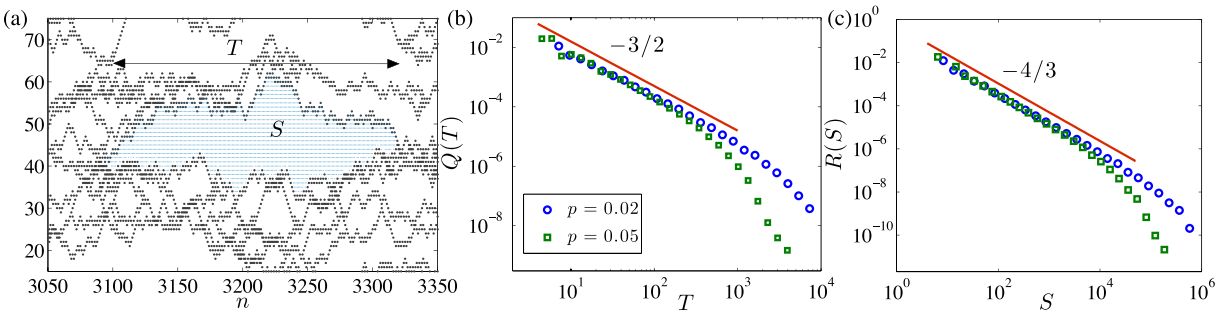

FIG. 8. (a) Voids are defined as closed regions of unoccupied sites, and they are defined by an area S (blue region) and duration T. (b),(c) Probability distribution function of the void durations and sizes, respectively, for two different values of p and $r = 0.01$. Solid red lines correspond to a power law with exponents $-3/2$ (b) and $-4/3$ (c).

The aggregation-fragmentation-diffusion process provides insight into the highly inhomogeneous distributions of particles advected by turbulent, compressible flows. Specifically, we refer here to a model of transport of inertial particles by a turbulent fluid [41–46],

$$\dot{x} = v,$$
$$\dot{v} = \mu[u(x,t) - v], \tag{25}$$

where μ is a constant, proportional to the fluid viscosity, describing the rate of damping of motion of a small particle relative to the fluid and $u(x,t)$ is the randomly fluctuating velocity field of the fluid in which the particles are suspended. The velocity is characterized by the correlations $\langle u(x,t)\rangle = 0$ and $\langle u(x,t)u(x',t')\rangle = C(x - x')\delta(t - t')$, where the angular brackets denote ensemble averages, and the function C is a Gaussian.

Numerical studies of (25) reveal particle trajectories that share many similarities with the trails displayed in Fig. 2: Particle trajectories may meander in space, merge, or split [26,27]. There are also strong quantitative similarities between the two models. The distribution of empty regions with area S in the space-time diagram defined in Fig. 8(a) is characterized by a power-law tail with an exponent $4/3$ [26], in agreement with Eq. (24). Further, the distribution of trajectories with weight w has a power-law tail as in (1) with a positive exponent γ. It would be interesting to explore further analogies between the aggregation-fragmentation-diffusion model and the theoretical model for particle transport by compressible turbulent flows. The resulting theoretical understanding could provide insight on experimental observations on the dispersion of particles on a surface flow [47].

ACKNOWLEDGMENTS

The authors are grateful to the Kavli Institute for Theoretical Physics for support, where this research was supported in part by the National Science Foundation under Grant No. PHY1125915.

[1] P. L. Krapivsky, S. Redner, and E. Ben-Naim, *A Kinetic View of Statistical Physics* (Cambridge University Press, Cambridge, U.K., 2010).
[2] R. D. Vigil, R. M. Ziff, and B. Lu, Phys. Rev. B **38**, 942 (1988).
[3] P. L. Krapivsky and S. Redner, Phys. Rev. E **54**, 3553 (1996).
[4] S. N. Majumdar, S. Krishnamurthy, and M. Barma, Phys. Rev. Lett. **81**, 3691 (1998).
[5] E. Ben-Naim and P. L. Krapivsky, Phys. Rev. E **77**, 061132 (2008).
[6] D. A. Lowe and L. Thorlacius, Phys. Rev. D **51**, 665 (1995).
[7] P. J. Blatz and A. V. Tobolsky, J. Phys. Chem. **49**, 77 (1945).
[8] R. Rajesh and S. N. Majumdar, Phys. Rev. E **63**, 036114 (2001).
[9] R. D. Vigil, J. Colloid Interface Sci. **336**, 642 (2009).
[10] A. E. Scheidegger, Water Resour. Res. **3**, 103 (1967).
[11] G. Huber, Phys. A (Amsterdam) **170**, 463 (1991).
[12] C. H. Liu, S. R. Nagel, D. A. Schecter, S. N. Coppersmith, S. Majumdar, O. Narayan, and T. A. Witten, Science **269**, 513 (1995).
[13] S. N. Coppersmith, C.-h. Liu, S. Majumdar, O. Narayan, and T. A. Witten, Phys. Rev. E **53**, 4673 (1996).
[14] P. J. Flory, J. Am. Chem. Soc. **63**, 3083 (1941).
[15] A. A. Lushnikov, J. Colloid Interface Sci. **65**, 276 (1977).
[16] R. M. Ziff, E. M. Hendriks, and M. H. Ernst, Phys. Rev. Lett. **49**, 593 (1982).
[17] P. G. J. van Dongen and M. H. Ernst, J. Stat. Phys. **49**, 879 (1987).
[18] F. Leyvraz, Phys. Rep. **383**, 95 (2003).
[19] A. F. Filippov, Theory Prob. Appl. **6**, 275 (1961).
[20] E. D. McGrady and R. M. Ziff, Phys. Rev. Lett. **58**, 892 (1987).
[21] Z. Cheng and S. Redner, J. Phys. A **23**, 1233 (1990).
[22] M. H. Ernst and G. Szamel, J. Phys. A **26**, 6085 (1993).
[23] P. L. Krapivsky and E. Ben-Naim, Phys. Rev. E **68**, 021102 (2003).
[24] R. M. Alexander, J. Avian Biol. **29**, 387 (1998).
[25] L. P. Brower and S. B. Malcolm, Am. Zool. **31**, 265 (1991).
[26] M. Pradas, A. Pumir, G. Huber, and M. Wilkinson, J. Phys. A **50**, 275101 (2017).
[27] G. Huber, M. Pradas, A. Pumir, and M. Wilkinson (unpublished).
[28] R. J. Glauber, J. Math. Phys. **4**, 294 (1963).
[29] Z. Rácz, Phys. Rev. Lett. **55**, 1707 (1985).
[30] M. D. Grynberg, T. J. Newman, and R. B. Stinchcombe, Phys. Rev. E **50**, 957 (1994).

[31] V. Privman and M. Barma, J. Chem. Phys. **97**, 6714 (1992).
[32] P. L. Krapivsky and E. Ben-Naim, J. Chem. Phys. **100**, 6778 (1994).
[33] X. Jin, G. Tarjus, and J. Talbot, J. Phys. A **27**, L195 (1994).
[34] C. Connaughton, R. Rajesh, and O. Zaboronski, Phys. Rev. Lett. **98**, 080601 (2007).
[35] V. E. Zakharov, V. S. Lvov, and G. Falkovich, *Kolomogorov Spectra of Turbulence I: Wave Turbulence* (Springer-Verlag, New York, 1992).
[36] E. Ben-Naim and J. Machta, Phys. Rev. Lett. **94**, 138001 (2005).
[37] S. Redner, *A Guide to First-Passage Processes* (Cambridge University Press, Cambridge, U.K., 2001).
[38] J. L. Spouge, Phys. Rev. Lett. **60**, 871 (1988).
[39] B. R. Thomson, J. Phys. A **22**, 879 (1989).
[40] M. A. Burschka, C. R. Doering, and D. ben-Avraham, Phys. Rev. Lett. **63**, 700 (1989).
[41] R. Gatignol, J. Méc. Théor. Appl. **2**, 143 (1983).
[42] M. R. Maxey and J. J. Riley, Phys. Fluids **26**, 883 (1983).
[43] G. Falkovich, K. Gawedzki, and M. Vergassola, Rev. Mod. Phys. **73**, 913 (2001).
[44] F. Toschi and E. Bodenschatz, Annu. Rev. Fluid Mech. **41**, 375 (2009).
[45] K. Gustavsson and B. Mehlig, Adv. Phys. **65**, 1 (2016).
[46] A. Pumir and M. Wilkinson, Annu. Rev. Condens. Matter Phys. **7**, 141 (2016).
[47] J. Larkin, M. M. Bandi, A. Pumir, and W. I. Goldburg, Phys. Rev. E **80**, 066301 (2009).